Electro-Magnetic Flow Control of Near-Wall Turbulence for Drag Reduction

Junguo Pang, Kwing-so Choi
School of Mechanical, Materials, Manufacturing Engineering and Management,
University of Nottingham, Nottingham, NG7 2RD, UK
eaxjgp@nottingham.ac.uk, kwing-so.choi@nottingham.ac.uk

ABSTRACT

Results from an experimental investigation of Electro-Magnetic Turbulent Control (EMTC) in an open water channel are presented in this paper. With better understanding of the regeneration cycle of near-wall turbulence events and coherent structures, most of the turbulent control strategies are focus on how to effectively disturb this regeneration cycle. Spanwise-wall Oscillation Turbulence Control (SWO-TC) is one of these strategies, which has been studied intensively in the past decade. Spanwise Oscillating Electro-Magnetic Turbulent Control (SO-EMTC) has been developed as a result of these investigations. To make the water electrically conductive, $CuSO_4$ solution was injected tangentially to the flow in the near-wall region of the boundary layer through a rectangular slot. The conductivity within the boundary layer over the test plate has to be known in order to obtain accurate Lorentz force distribution on the EMTC arrays. Two different methods to get this concentration/conductivity profile were presented in this paper.

Our experimental data shows that the mean velocity gradients and the turbulence intensities in the near-wall region were reduced and the increases of higher moments of turbulence statistics like skewness and kurtosis near the wall suggested the thickness of viscous sublayer was increased by SO-EMTC. 45% skin friction drag could be achieved when $St=30\pi Re_\tau/T^+=280$ in the present SO-EMTC conditions.

An "equivalent spanwise wall velocity" W^+_{equi} of SO-EMTC, which is considered as a bridge to connect SO-EMTC and SWO-TC together, was obtained from our calculation. The optimum Stuart number $St_{opt}=30\pi Re_\tau/T^+$ derived from this W^+_{equi} was found slightly greater than the DNS results. Both of our experimental data and calculation suggested that $St=30\pi Re_\tau/T^+$ is more likely to be the optimum St for SO-EMTC.

1. INTRODUCTION

From recent development in the study of the structure of turbulent boundary layer, the strategies for drag reduction could be generalised like this: Because the turbulent events in boundary layers are quasi-periodic, self-regenerating, the energy-production process of turbulent boundary layers can be modified if one part of the sequence of near-wall activities is disturbed (Choi 1996; Karniadakis and Choi 2003). Based on this idea, many new techniques for drag reduction have been developed in the last decade, including riblets (Walsh 1989; Choi 1989), spanwise wall oscillation (Jung, Mangiavacchi et al. 1992; Laadhari, Skandaji et al. 1994; Choi, DeBisschop et al. 1998; Dhanak and Si 1999) and spanwise travelling wave (Du and Karniadakis 2000), etc. Among these techniques, Spanwise-wall oscillation Turbulent Control (SWO-TC) is one of the most effective ways to disturb this sequence. Over the last ten years, it has been studied by many researchers (Jung, Mangiavacchi et al. 1992; Laadhari, Skandaji et al. 1994; Baron and Quadrio 1996; Dhanak and Si 1999; Quadrio and Sibilla 2000; Choi 2002) both in DNS and in experimental studies. It was shown that up to 45% skin-friction drag reduction could be achieved when the oscillating nondimensional period T^+ is around 100. Such a high potential for drag reduction led the spanwise-wall oscillation research to one of the most popular study topics for turbulence in the last decade. To understand the mechanism of spanwise-wall oscillation, Choi et al. carried out a series of experimental research by using hot-wire anemometory and flow visualization study of the near-wall turbulence structures over the oscillating wall (Choi et al. 1998; Choi and Clayton 2001; Choi 2002). It was shown that the turbulent skin-friction reduction with spanwise-wall oscillation can be optimized with a non-dimensional spanwise wall velocity W_0^+, and nearly 45% drag reduction can be obtained in the turbulent boundary layer at an optimum value of $W_0^+=15$.

The Lorentz force, generated by the electromagnetic fields, which can act upon the conducting liquid in the form of a body force, is believed to have potential for turbulent boundary control and drag reduction (Berger, Kim et al. 2000). This idea has been recognised for a long time, but it became popular only in the last five years. Using Lorentz body force for flow control: it is easy to produce some flow control strategies such as wall normal jet/suction, streamwise blow or spanwise oscillation by only simply altering the arrangement of electrodes and polarities of the magnets without changing the boundary wall. Among all of the EMTC techniques, Spanwise Oscillating Electro-magnetic Turbulence Control (SO-EMTC) has drawn our attention. At the same time, the electric-chemical reaction on the electrodes (bubbles and deposits of metals) can be greatly reduced by periodically change the polarities of electrodes. For SO-EMTC study, Berger et al. from UCLA group have presented a very detailed DNS study for different oscillating frequency at different Reynolds number (Berger, Kim et al. 2000). It was found that the optimal oscillatory frequency T^+ around 100 could apply for a wide range of Reynolds number. But in order to achieve maximum drag reduction, two necessary conditions have to be satisfied: First, the shear layer generated by the Lorentz force must be applied in a location where the streamwise vortices are found. The centres of the streamwise vortices are located approximately $y^+=15$-25 away from the wall, so the penetration depth $\Delta^+=a^+/\pi$, where a is the electrode and magnet width, has to be set to a value to make sure the Lorentz force still has effect up to 30 wall unit. Here Δ^+ was set to 10 based on the model of Berger and Kim et al; Second, the Lorentz force has to be large enough to modify the near-wall turbulence structures. In other words, the amplitude of the oscillation has to be big enough to effectively suppress the streamwise

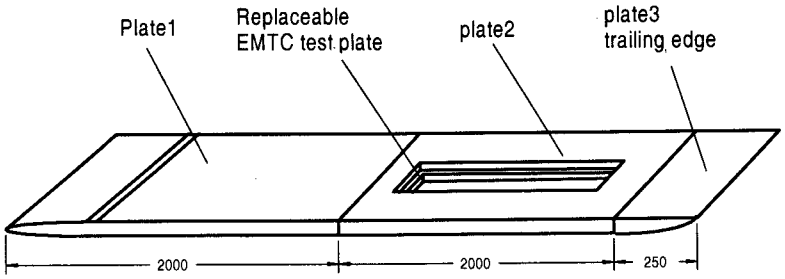

Figure 1 Test plate of the experiments with dimensions

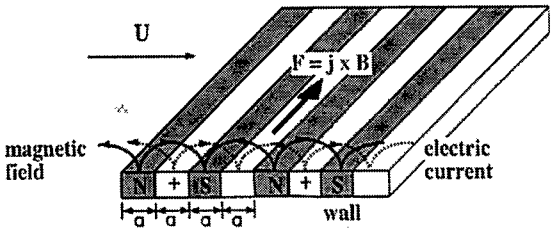

Figure 2. Configuration of electrodes and magnets to create Lorenz in parallel to wall surface, normal to flow direction.By switching the polarity of the electric current, spanwise-oscillating Lorenz force field was created.

vortices (Berger, Kim et al. 2000). So the oscillating magnitude of the Lorentz force has to increase proportionally to the Reynolds number. In Berger et al.'s DNS paper, after simplifying the mean spanwise velocity equations, an optimum Stuart number St [$St=(J_0B_0\delta)/(\rho u_\tau^2)$, which is the ratio of the Lorentz force to the inertia force of the fluid], has been given by the following equations:

$$\left(\frac{StT^+}{\mathrm{Re}_\tau \pi}\right)_{opt} \approx 20 \qquad (1)$$

SO-EMTC and SWO-TC seems to work in different mechanism near the wall although they do have many similarities: SO-EMTC is driven by a shear layer generated by Spanwise Oscillating Lorentz body force, therefore the maximum spanwise velocity is away for the wall; On the other hand, SWO-TC is driven by the near-wall Stokes Layer, so the maximum spanwise velocity is on the wall due to the non-slip condition.

To better understand the mechanism of SO-EMTC, visualisation experiments to show the changing of near-wall streaks in the condition of with and without SO-EMTC were done by adding dye or $KMnO_4$ in the $CuSO_4$ solution. The visualisation pictures (see figure 3) shows that the streak structure in the near-wall region is greatly altered (the picture shows that the streaks are moved upward) due to the spanwise oscillating Lorentz force.

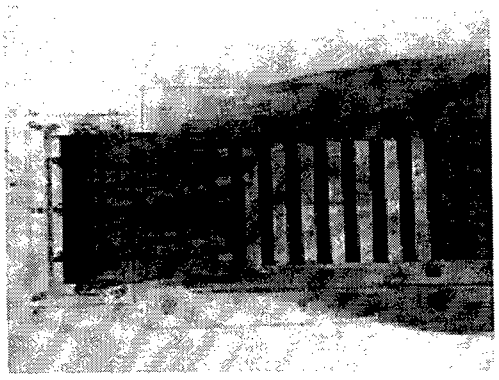

Figure 3. Flow visualisation of turbulent boundary layer with spanwise-oscillating Lorenz force.

Corrosion is a very serious problem for EMTC especially for seawater channel. The working solution in our experiments was chose as $CuSO_4$ instead of seawater. $CuSO_4$ solution was injected tangentially into the flow through a rectangular slot to make the water electrically conductive in the near-wall region of the boundary layer. But the concentration of the $CuSO_4$ near the wall will decrease with x after convecting further downstream. In order to accurately estimate the Eletro-magnetic (Lorentz) force distribution over the EMTC actuators, the concentration/conductivity distribution of the injected $CuSO_4$ has to be measured. The techniques to measure the $CuSO_4$ concentration are presented in Section 3.1.

Hot-film anemometry was used throughout the experiments. The velocity field and associated statistics of the turbulent boundary layer by SO-EMTC for different St were presented in Section 3.2. In Section 3.3 of this paper, an "equivalent spanwise wall velocity" W^+_{equi} was derived from the similarity in the spanwise velocity profile between the Spanwise wall oscillation (SWO-TC) and the Lorentz force oscillation (SO-EMTC). The optimum $St=30\pi \mathrm{Re}_\tau/T^+$ derived from this W^+_{equi} is similar to the optimum St from Berger et al's DNS results, and the experimental data shows good agreement with Choi's SWO-TC results (Choi, DeBisschop et al. 1998).

2. EXPERIMENTAL SETUP

The present experiments were performed in a 7.3 meter long open water channel with a working section of 600mm × 300mm. Water is pumped from the downstream tank to the up-stream tank via a pipe system outside of the channel and the total flux is controlled by the main valve just before the pump and bypass valve just after the pump. At the same time, water depth and flow speed in the channel can be controlled by the gates in the downstream of the channel. A 4-meter long test plate with 20:1 ellipse leading edge was placed in the channel (Figure 1). The boundary layer was tripped just after the leading edge to ensure a fully developed turbulent boundary layer over the working area on the test plate. The test plate material is made of perspex with a replaceable part for EMTC control actuators and $CuSO_4$ injection slot to fit in. The turbulent intensity in this open-channel has been reduced to approximately 2% by placing screens and honeycombs in the channel and up-stream tank just before the test plate. The freestream velocity of the present experiments is set to 0.16 m/s, with a nearly zero pressure gradient along the length of the working section.

Single component stremwise velocity measurements were made by Dantec 56C CTA system and a single, miniature boundary type hot-film probe-Dantec 55R15. This

Table 1. Experimental conditions and flow parameters.

Re_τ	Δ^+	u_τ [m/s]	U_∞ [m/s]	J_0[A/m^2]	V_0 [v]	B_0 [T]	St	F
300	10	0.0068	0.16	320	7	0.8	180-400	0.094

fiber-film sensor is a Nickel film deposited on a 70μm diameter quartz fiber. Overall length is 3 mm, and sensitive film length is 1.25 mm. Film is protected by a quartz coating approximately 2 μm thickness, which can protect the film to work in this conductive and corrosive solutions after $CuSO_4$ injection in the systems. The hot-film was operated in constant temperature mode (except when we are measuring the concentration profile by hot-water injection, CCA mode was used in this measurement). The over-heat-ratio of the film was set to 1.05, which can effectively reduce the bubbles generation from the film surface. Data from the anemometer system were sampled at a rate of 50 Hz using an IOTech ADC 488/8S analogue-to-digital (AD) converter. The probe is mounted to a wall normal (y-axis) traverse system, which is computer controlled via a Digiplan step-motor controller. The wall normal movements are made with a resolution of 1.25 μm.

The EM actuators, which are placed within the replaceable test surface, are made up by fitting permanent magnets-Neodymium Iron Boron Magnets (NdFeB) with 1.2T and electrodes (made of Copper) side by side (Figure 2). The effects of spanwise-oscillating Lorentz force, can be achieved by switching the polarity of the electric current periodically. The oscillation frequency was set by an optimum value for spanwise-wall oscillation corresponding to the non-dimensional period T^+=100. Experimental conditions and flow parameters are summarised in Table 1.

During the experiments, Copper (Cu), one of the productions of the electro-chemical reaction in the $CuSO_4$ solution, will be deposited on the Copper electrodes without changing the surface characters of the electrodes. The total area of the EMTC is made up by 16 small Electro-magnetic arrays, which will cover x^+ up to 3000 downstream of the injection slot and z^+ up to 1200. To avoid any possible Electro-magnetic interference with the hot-film, the measurements were confined at the downstream of the electro-magnetic test plate. The $CuSO_4$ solution was injected tangentially to the near-wall region through a 0.5mm wide and 250mm long slot. From this injection, a suitable layer with strong conductivity is produced just above the EM surface without soiling the rest of water. The present injection slot can also served as a hot water injection system as one of the methods to indirectly measure the concentration profile of $CuSO_4$. Dantec 56C20 Temperature Bridge was chosen to do the temperature measurement running at constant current (CCA) module. Again Dantec 55R15 fiber-film sensor was used as the temperature wire because it is very robust and suitable for using in water. This cold wire temperature measurement is very linear and accurate with temperature dependent input drift 3μV/°C.

3. RESULTS & DISCUSSIONS

3.1 Concentration Measurement

In order to accurately estimate the Lorentz force distribution over the Electro-magnetic arrays on the test plate, the conductivity/concentration distribution of the injected $CuSO_4$ has to be known. In this section, we present two methods to measure the concentration of injected $CuSO_4$: one by taking sample directly from a sampling tube and another by indirectly measuring the relative temperature distribution of hot water injecting from the slot. Hot water of about 3 °C higher than the channel water was injected from the injection slot for the measurement.

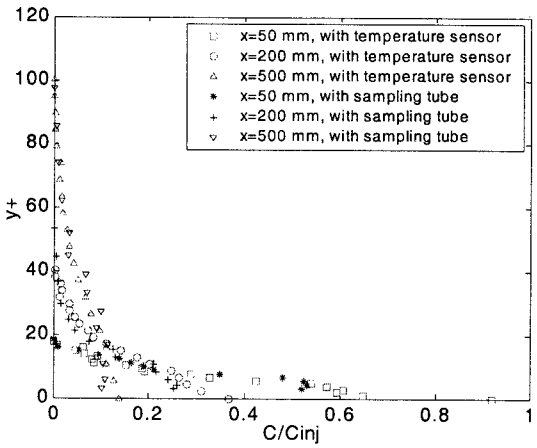

Figure 4. Concentration profiles measured by temperature sensor and small sampling tube at three different x positions

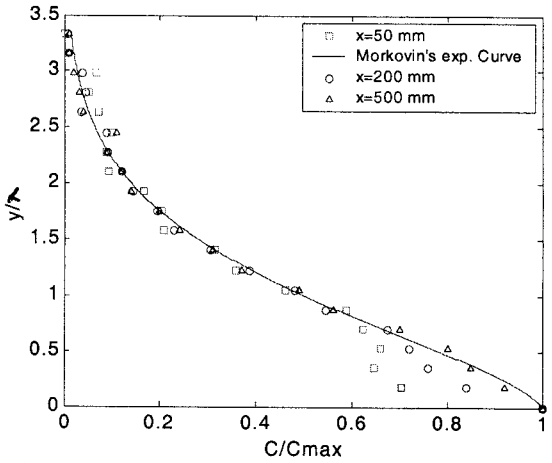

Figure 5 Comparison of the normalized mean concentration profiles at three different x positions with the empirical curve from Morkovin (1965)

Figure 4 is the concentration profiles at 3 different x position downstream of the slot. It is clearly shown that the concentration on the wall decreases as the solution convect further downstream. At the same time, the thickness of the diffusive boundary layer increases with x. When measuring point is very close to the injection slot (x=50 mm in Figure 4), the diffusive boundary layer thickness is very thin and the near-wall concentration gradient is very high. The comparisons of these two different methods--temperature sensor and tube sampling method are also shown in the figure. It can be seen that these two methods show a good agreement away from the wall, but close to the wall, the wall

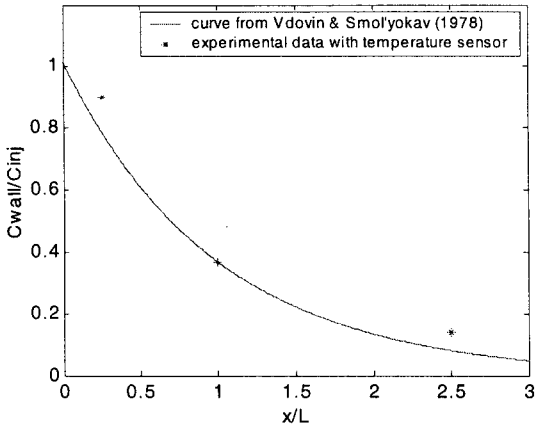

Figure 6. Near-wall concentration decreasing with the increasing streamwise distance downstream of the injection slot

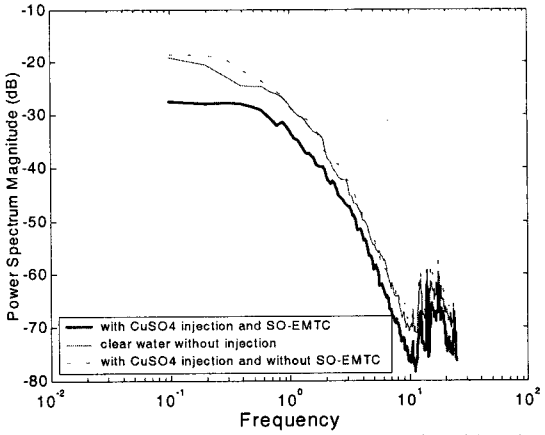

Figure 7. Energy spectrum of u-component velocity with and without SO-EMTC

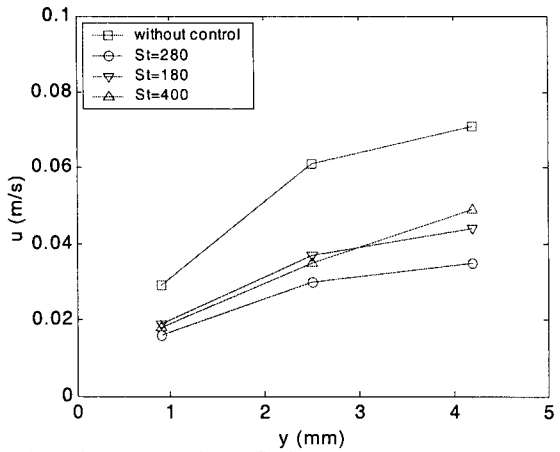

Figure 8. Mean velocity profile in the near-wall region without and with SO-EMTC at different St numbers

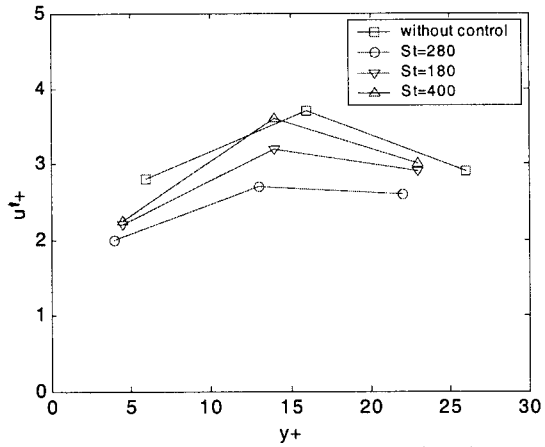

Figure 9. Turbulence intensity in the near-wall region without and with SO-EMTC at different St numbers

effect becomes significant: the concentration results from the sampling tube method in this area tend to give a lower value as compared to the water injection method. The advantage of using water injection method is that we can get the concentration profile very close to the wall while for the sampling tube method, the nearest y position for the sampling to the wall is 1/2 outer diameter of the tube.

Our experimental data suggests that the diffusion of $CuSO_4$ is similar to the diffusion of a passive contaminant from a line source onto a flat-plate. Figure 5 is the normalized mean concentration profiles at three x positions. The comparison with Morkovin's curve, an empirical curve for the diffusion of a passive contaminant and polymers from a line source onto a flat-plate is also shown in the figure (Morkovin 1965). Based on the range of λ/δ, four diffusive zone was identified downstream of the injector: initial ($\lambda/\delta<0.1$), intermediate ($0.1<\lambda/\delta<0.39$), transition ($0.39<\lambda/\delta<0.64$) and final diffusion zone ($\lambda/\delta=0.64$), where λ is the diffusion boundary-layer thickness, defied as the distance from the wall at which the mean concentration drops to 50% of its maximum concentration at a given streamwise measurement location and δ is the local boundary layer thickness (Morkovin 1965; Wu and Tulin 1972; Lumley 1973). Since Morkovin's curve is only suitable for intermediate zone and downwards, from Figure 5, it was shown that at x=500 mm downstream of the slot, the diffusive boundary layer has developed to intermediate zone ($\lambda/\delta=0.12$), and at both x=50 and x=200 mm, the diffusion boundary layers have not developed to intermediate zone yet because the concentration gradients in the near-wall region are still high.

Figure 6 is another view of the wall concentration change with x. The trend shows good agreement with the results of Vdovin & Smol'yokav's water injection data (Wu and Tulin 1972).

3.2 Results of Boundary Layer Profile Data Under SO-EMTC

In the present research, we fixed the $T^+=100$, penetration depth $\Delta^+=10$ and $Re_\tau=300$. (more detailed investigation of different T^+, Re_τ and Δ^+ is currently being carried on.) Three different *St* numbers-180, 280 and 400 were chosen for the SO-EMTC test, which are corresponding to $20\pi Re_\tau/T^+$, $30\pi Re_\tau/T^+$ and $40\pi Re_\tau/T^+$ respectively under the present experimental condition. Considering the corrosion of the channel water to the probe and channel systems, the boundary profile was taken at some character points after comparing the boundary layer profile with and without SO-EMTC. Here, the velocity measurements were taken at $y^+=5$, 15 and 25.

The energy spectrum of *u*-velocity fluctuations measured within the viscous sublayer (figure 7) indicates a large reduction in the energy by oscillating Lorentz force, particularly at low frequencies. The *u* spectrum of with injection but without oscillation was also shown, suggesting that the effect on the boundary layer structure due to injection is negligible.

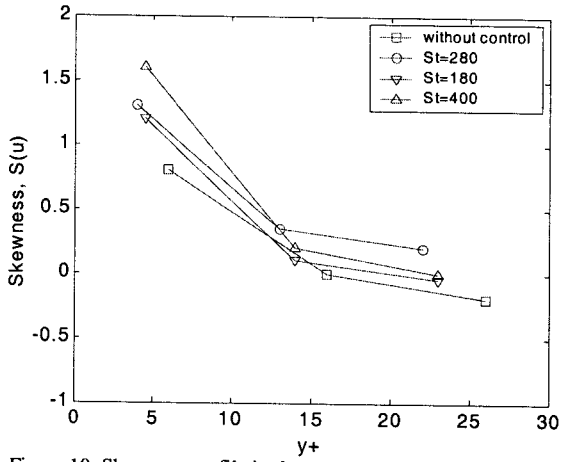

Figure 10. Skewness profile in the near-wall region without and with SO-EMTC at different St numbers

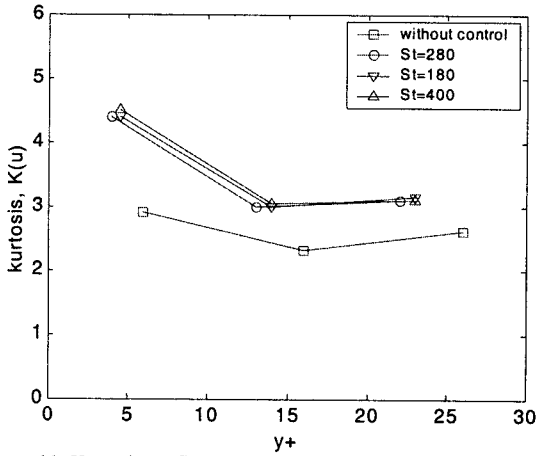

Figure 11. Kurtosis profile in the near-wall region without and with SO-EMTC at different St numbers

Figure 8 is the mean velocity profile in the near-wall region for non-control condition and with SO-EMTC under different St numbers. For all the values of St tested in the present experiments, the near-wall velocity slopes were reduced. It can be seen that when St=280, the near-wall velocity gradient shows as much as 45% reductions in skin friction drag while both St=180 and 400 have about 35% skin friction reduction.

It was also shown that the near-wall turbulence intensities were reduced with SO-EMTC (figure 9). When St=280, the turbulence intensity at the near-wall region (y^+=5 and 15) could be reduced by 30%. For St=180 and 400, the turbulence intensity reduction are slightly less at y^+=5. But for St=400 at y^+=15, the turbulence intensity is close to the flow intensity without control, indicating that the spanwise disturbance to the near-wall turbulent structures has passed the optimum value and tend to give negative influence. From the analyses of figure 8 and figure 9, it suggests that $St=30\pi Re_\tau/T^+=280$ is more likely to be the optimum St for SO-EMTC.

The distribution of skewness and kurtosis of the velocity fluctuation are presented in figure 10 and figure 11, respectively. Both of these higher moments of turbulence statistics seem to increase within and just outside the viscous sublayer, suggesting the increases in the viscous sublayer thickness by SO-EMTC. These agree well with the DNS results (Baron and Quadrio 1996) as well as the experimental results (Choi, DeBisschop et al. 1998) for SWO-TC.

3.3 *w* Velocity Calculation and Comparison Between SWO-TC and SO-EMTC

Both SWO-TC and SO-EMTC can generate a periodic oscillating shear layer in the near-wall region. They do have many similarities. As mentioned in Section 2, these shear layers must have thick enough penetration depth so that these shear layers could disturb the near-wall quasi-streamwise vortices effectively. The centres of the quasi-streamwise vortices are located approximately y^+=15-25 away from the wall, so the penetration depth $\Delta^+=a^+/\pi$, where a is the electrode and magnet width, has to be set to a value to make sure the Lorentz force still has effect up to 30 wall unit (Berger, Kim et al. 2000). In the present SO-EMTC research, Δ^+=10, with the effective Lorentz force could work up to 30 wall unit (about 5% of the Lorentz force on the wall at y^+=30). Choi also mentioned that a similar penetration depth in his SWO-TC results; T^+, a non-dimensional period of the oscillating shear layer, has to be optimised in order to match the rhyme of the quasi-periodic and self-regenerating near-wall events. Optimum T^+ was found around 100 for both the SWO-TC and the SO-EMTC.

Apart from optimum Δ^+ and T^+, for SWO-TC, it has been shown that the spanwise velocity profile over a spanwise oscillating wall is nearly identical to the theoretical laminar velocity profile over an oscillating plate in still fluid both by DNS and experimental results (Jung, Mangiavacchi et al. 1992; Laadhari, Skandaji et al. 1994; Baron and Quadrio 1996; Dhanak and Si 1999; Quadrio and Sibilla 2000; Choi 2002) The non-dimensional form of this spanwise velocity w^+, is given by the following Stokes solutions:

$$w^+=W_0^+\exp[-y^+(\pi/T^+)^{1/2}]\cos(2\pi t^+/T^+) \qquad (2)$$

Equation (2) shows that the spanwise velocity in the Stokes Layer reduces exponentially as y^+ increases.

For SO-EMTC, on the other hand, the shear layer is driven by a spanwise oscillating Lorentz body force where the maximum spanwise velocity is located away from the wall although the maximum Lorentz force is at the wall. This oscillating Lorentz force has to be strong enough to give spanwise disturbance to the near-wall structures.

So, finding the similarities in the spanwise velocity profiles between the SWO-TC and SO-EMTC is crucial if we want to link these two control strategies together.

When a Lorentz body force was applied for a laminar flow, the equation for the mean spanwise velocity was given by (Berger, Kim et al. 2000).

$$\frac{\partial W^+}{\partial t^+}=\frac{\partial^2 W^+}{\partial y^{+2}}+\frac{St}{\mathrm{Re}_\tau}\exp\left(-\frac{y^+}{\Delta^+}\right)\sin\left(\frac{2\pi\cdot t^+}{T^+}\right) \qquad (3)$$

The solution of equation (3) indicated that w^+ reaches the maximum velocity at about 3/4 of the penetration depth Δ^+, which is about y^+=7.5 for the current Δ^+=10, then it starts to decrease exponentially. From $y^+>3/4\Delta^+$, our calculations shows that the $\partial^2 W^+/\partial y^{+2}$ term in Equation (3) is very small (less than 5%) as compared to the second term on the left hand side of Equation (3). Therefore, the spanwise velocity equation for SO-EMTC could be simplified as an ordinary differential equation for $y^+>3/4\Delta^+$:

$$\left.\frac{dW^+}{dt^+}\right|_{y^+>3/4\Delta^+}=\frac{St}{\mathrm{Re}_\tau}\exp\left(-\frac{y^+}{\Delta^+}\right)\sin\left(\frac{2\pi\cdot t^+}{T^+}\right) \qquad (4)$$

And the solutions can be given by

$$W^{+}{}_{y^{+}>3/4\Delta^{+}} = \frac{StT^{+}}{\mathrm{Re}_{\tau}\,2\pi}\exp\left(-\frac{y^{+}}{\Delta^{+}}\right)\cdot\left[-\cos\left(\frac{2\pi\cdot t^{+}}{T^{+}}\right)\right] \quad (5)$$

Which is similar to the Stokes solutions in equation (2).

Comparing equation (5) with equation (2), we found that $StT^{+}/(2\pi Re_{\tau})$ can be taken as an equivalent non-dimensional "spanwise wall velocity" under the conditional of SO-EMTC. Actually this "equivalent spanwise wall velocity" can also be found if we extend the outer region of exponential distribution of w^{+} (equation 5) to the wall.

$$W^{+}{}_{equi} = \frac{StT^{+}}{2\pi\,\mathrm{Re}_{\tau}} \quad (6)$$

If we using the optimum $St=20\pi\mathrm{Re}_{\tau}/T^{+}$ suggested by Berger et al (2000), we can find a $W^{+}{}_{equi}=10$ for SO-EMTC, which is close to the optimum spanwise wall velocity for SWO-TC, $W_0{}^{+}=15$. (Choi and Clayton 2001; Choi 2002)

But if we take the optimum $W^{+}{}_{equi}=W_0{}^{+}=15$, we can find a new optimum St number for SO-EMTC:

$$St_{opt} \approx \frac{30\pi\cdot\mathrm{Re}_{\tau}}{T^{+}} \quad (7)$$

Which is slightly bigger than the optimum $St=20\pi\mathrm{Re}_{\tau}/T^{+}$ from Berger's DNS results (Berger, Kim et al. 2000).

From the experimental results of Section 3.2, it seems that when $St=30\pi\mathrm{Re}_{\tau}/T^{+}=280$, 45% skin friction reduction could be achieved while $St=20\pi\mathrm{Re}_{\tau}/T^{+}=180$, we can get about 35% drag reduction. Our calculation here has confirmed that $St=30\pi\mathrm{Re}_{\tau}/T^{+}$ is more likely to be the optimum St for SO-EMTC. It seems that this $W^{+}{}_{equi}$ is an effective bridge to link SO-EMTC and SWO-TC together.

4. CONCLUSIONS

In this paper, concentration/conductivity profile of the injected CuSO4 was measured first in order to get the Lorentz force distribution on the EMTC test arrays. Our experimental data shows that the diffusion of $CuSO_4$ is similar to the diffusion of a passive contaminant from a line source onto a flat-plate. Two methods to measure the concentration of injected $CuSO_4$ were presented: one by taking sample directly from a sampling tube and another one by measuring the relative temperature distribution of hot water injecting from the slot. It can be seen that these two methods show a good agreement in the outer region of the diffusion boundary layer. But close to the wall, the concentration results from the sampling tube method tends to give a lower value because of the wall effect. By using the water injection method, we can get the concentration profile very close to the wall while for the sampling tube method, the nearest y position for the sampling to the wall is only 1/2 outer diameter of the tube.

By measuring the velocity profiles in the near wall region with and without SO-EMTC, it was shown that the mean velocity gradients and the turbulence intensities in the near-wall region were reduced and the increases of higher moments of trubulence statistics like skewness and kurtosis near the wall suggested the increases in the viscous sublayer thickness by SO-EMTC. 45% skin friction drag could be achieved when $St=30\pi\mathrm{Re}_{\tau}/T^{+}=280$ in the present experimental conditions. Our experimental data of SO-EMTC shows good agreement with Choi's experimental results of SWO-TC.

We successfully built up the link between SO-EMTC and SWO-TC through an "equivalent spanwise wall velocity" $W^{+}{}_{equi}=StT^{+}/(2\pi\mathrm{Re}_{\tau})$ for SO-EMTC. When $W^{+}{}_{equi}$ was set equal to the optimum $W_0{}^{+}=15$ for SWO-TC, an optimum $St_{opt}=30\pi\mathrm{Re}_{\tau}/T^{+}$ for SO-EMTC can be derived and this value is similar to Berger et al's DNS solution, in which the optimum $St_{opt}=20\pi\mathrm{Re}_{\tau}/T^{+}$. Both of our experimental data and calculation suggested that $St=30\pi\mathrm{Re}_{\tau}/T^{+}$ is more likely to be the optimum St for SO-EMTC.

REFERENCES

Baron, A. and M. Quadrio (1996). "Turbulent drag reduction by spanwise wall oscillations." *Appl. Sci. Res.* **55**: 311.

Berger, T. W., J. Kim, et al. (2000). "Turbulent boundary layer control utilizing the Lorentz force." *Phys. Fluids* **12**(3): 631-649.

Choi, K.-S. (1989). "Near-wall structure of a turbulent boundary layer with riblets." *J. Fluid Mech.* **208**: 417-458.

Choi, K.-S. (1996). Turbulent drag reduction strategies. *Emerging Techniques in Drag Reduction*. K.-S. Choi, K. K. Prasad and T. V. Truong. London, MEP: 77-98.

Choi, K.-S. (2002). "Near-wall structures of turbulent boundary layer with spanwise-wall oscillation." *Phys. Fluids* **14**: 2530.

Choi, K.-S. and B. R. Clayton (2001). "The mechanism of turbulent drag reduction with wall oscillation." *Int. J. Heat and Fluid Flow* **22**: 1.

Choi, K.-S., J.-R. DeBisschop, et al. (1998). "Turbulent boundary-layer control by means of spanwise-wall oscillation." *AIAA Journal* **36**(7): 1157-1163.

Dhanak, M. R. and C. Si (1999). "On the reduction of turbulent wall friction through spanwise oscillations." *J. Fluid Mech.* **383**: 175-195.

Du, Y. and G. E. Karniadakis (2000). "Suppresing wall turbulence by means of tranverse traveling wave." *Science* **288**: 1230.

Jung, W. J., N. Mangiavacchi, et al. (1992). "Suppression of turbulence in Wall-bounded flows by high-frequency oscillations." *Phys. Fluids A* **4**(8): 1605-1607.

Karniadakis, G. E. and K.-S. Choi (2003). "Mechanisim on transverse motions in turbulent wall flows." *Annu. Rev. Fluid Mech.* **35**: 45-62.

Laadhari, F., L. Skandaji, et al. (1994). "Turbulence reduction in a boundary layer by a local spanwise oscillating surface." *Phys. Fluids* **6**: 3218.

Lumley, J. L. (1973). "Drag reduction in turbulent flow by polymer addictives." *J. Polymer Science. Macromolecular Rev.* **7**: 283-290.

Morkovin, M. V. (1965). "On eddy diffusivity, quasisimilarity and chemical reactions in turbulent boundary layers." *Int. J. Heat Mass Transfer* **8**: 129-145.

Quadrio, M. and S. Sibilla (2000). "Numerical simulation of turbulent flow in a pipe oscillating around its axis." *J. Fluid Mech.* **424**: 217.

Walsh, M. J. (1989). Riblets. *Viscous Drag Reduction in Boundary Layers, Progress in Astronautics and Aeronautics*. D. M. Bushnell and J. N. Hefner, AIAA. **123**.

Wu, J. and M. P. Tulin (1972). "Drag reduction by ejecting addictive solutions into a pure water boundary layer." *Trans. ASME. J. Basic Engng* **94**: 749-755.